ORIGINAL PAPER

Monitoring the changes in the dynamic properties of an RC building experiencing column loss

Fuat Aras[1] · F. Necati Çatbaş[2]

Abstract

In this study, an existing six-storey reinforced concrete building with an asymmetric structural plan and soft storey irregularity was used as a test specimen and subjected to three-step progressive structural damages to detect the variations in its dynamic properties. Mode shapes and dominant frequencies of the undamaged building were determined by the ambient vibration survey (AVS) and it was seen that its first three modes were torsion coupled. Besides, soft storey irregularity was evident due to the lack of masonry infill walls on its ground floor. Later on, three-step progressive damages were applied to the building. The first step targeted three columns and one beam of the building, located on a corner region of its ground floor to peel off their clear covers. The second step razed two adjacent corner columns which were already moderately damaged in the first step, while the third step knocked the third moderately damaged column down. After each damage step, AVS was repeated with the same details as applied for the undamaged building. The obtained dynamic properties for the four phases of the building were evaluated with the sustained damage. Numerical analyses with the finite element model of the building representing its four different phases were also performed and the unique responses due to damage effects on the structure were investigated numerically. As a result of induced damage, the quantified amount of frequency change in modes and the new mode observed after particularly column loss scenarios can be utilized for efficient structural health-monitoring strategies of plan-asymmetric buildings and post-earthquake assessment of partially damaged buildings where timely objective assessment is important.

Keywords AVS · OMA · Modal testing · Full-scaled experiment · Asymmetric plan · Soft storey

1 Introduction

1.1 Background of the study

More than 90% of Turkey's building stock consists of multi-storey reinforced concrete residential apartment buildings [1]. A large number of these buildings in the epicentre regions collapsed [2]. Indeed, Kocaeli and Düzce earthquakes (1999) are the milestones for the earthquake awareness of the Turkish community due to the life and economic losses they caused. These highlighted the need for seismic risk assessment of existing building stock. Henceforth, two validated seismic codes [3, 4] included a detailed chapter devoted to the seismic assessment of existing buildings in Turkey. Furthermore, the physical obsolescence and increased comfort expectations of the inhabitants forced the owners to renew their buildings. Indeed, the overall replacement of an old and underperforming building by a new one is affordable, since these buildings are mostly located in central locations. In these conditions, in 2012, the Law about the Transformation of the Areas under Disaster Risk [5] was released officially to pave the way for building reconstruction projects. After the validation of the LTADR, many buildings whose seismic performance had been assessed as inadequate were replaced by new buildings.

This study was performed over one of those buildings located in the Kadıköy District of Istanbul with its symmetrical twin. The building was used in two extensive research studies before. Aras et al. [6] applied AVS and parametric analyses to compare the modelling techniques for masonry

✉ Fuat Aras
fuat.aras@medeniyet.edu.tr

1   Civil Engineering Department, Istanbul Medeniyet University, Kuzey Yerleşkesi, Ünalan Mahallesi, F Blok, No: 133, Üsküdar, 34732 Istanbul, Turkey

2   Civil and Environmental Engineering Department, University of Central Florida, Orange County, Orlando, FL, USA

🖄 Springer

infill walls under low-amplitude vibration. In another study, Aras et al. [7] applied the AVS to the original and an altered form, obtained by demolishing all infill walls on the ground floor of the building. The authors also conducted numerical investigations with a validated finite element model of the building to search the effects of masonry infill walls on the dynamic properties of reinforced concrete buildings. The mentioned altered building was used in this study to search the effects of structural damages on the dynamic properties of reinforced concrete buildings.

Three progressive damage steps were applied to its three columns and one beam located on the ground floor of the building by applying destructive impacts with a construction-demolishing machine. In the first step, the impacts aimed to peel the clear cover of the members. This stage is called moderate damage (MD), while the second stage is called heavy damage-I (HD-I) and razed two moderately damaged corner columns. Finally, the third stage razed the last moderately damaged column and is called heavy damage-II (HD-II). At each step AVSs were performed; thereby the dynamic properties of the building were determined experimentally. Besides, by using the calibrated numerical model of the building, eigenvalue analyses were performed. Finally, the experimental and numerical dynamic properties of the undamaged and three damaged phases of the building were compared and discussed.

1.2 Brief review of relevant studies

The performed literature survey showed that the investigation of the effects of similar structural damages given in this study is a crucial subject that attracts the attention of the community. Earthquakes, terrorist attacks, vehicle crashes, or some other accidental events can be shown as the reasons for the partially damaged buildings. In this context, the effects of structural member loss were studied extensively. The partial collapse of the Murrah Federal Building was studied by Sozen et al. [8] and Kazemi-Moghaddem and Sasani [9]. These two studies resulted in different conclusions about the role of a key column in its loss. Parisi and Scalvenzi [10] numerically investigated the effects of different column loss scenarios for RC frames. The authors underlined the difference between the simultaneous and sequential removal of two columns for the load capacity. El-Demerdash et al. [11] investigated the effects of column loss in flat-plate RC buildings with nonlinear finite element analysis. The importance of bottom reinforcement in column strips is validated.

Presenting the results of full-scaled experimental research, the performed study also contributes to the literature on structural health monitoring. The changes in the global dynamic behaviour are studied for the health monitoring of civil structures [12]. In the early studies, the

frequency change was grasped as the "vibration signature" for the damage evaluation [13–16], while recently the evaluation performed with mode shape and damping properties was employed for plates, beam-like structures, bridges, planar trusses, and parabolic arches [17–23]. Recently, the experimental researches performed on real-life structures have attracted attention. Sampaio et al. [24] proposed the frequency response function curvature method and demonstrated its effectiveness on the Interstate-40 (I-40) bridge over the Rio Grande in Albuquerque, NM, USA. Since the bridge was planned to be razed, permission for destructive tests was given by the authorities. In another study, Catbaş et al. [25] proposed the use of modal flexibility function for the condition assessment and damage identification of bridges by proving the proposal in two real-life bridges in the USA. Dilena and Morassi [26] tested the Dogna Bridge in Italy. The authors presented six-level damage to the bridge to investigate the effects of incremental damage on its dynamic properties. It was concluded that the changes in modal curvature indicate the damage location. The given summary on the pre-completed studies can be extended, but the review articles [12, 24, 27–29] gave further details about the literature.

The literature survey also shows that there are a limited number of studies investigating the effects of damage on the dynamic properties of building-type structures. Most studies present parametric investigations performed on frames and shear buildings [30–32]. Recently, Bernagozzi et al. [33] proposed the use of a modal flexibility-based approach for damage detection and localization in buildings. The analytical results were controlled by vibration tests performed on a scaled four-storey symmetric steel frame structure in the laboratory. Wang et al. [34, 35] performed numerical and experimental studies. They used the vibration records gathered from a small-scale laboratory specimen, made of steel, representing a two-storey building with an 800 mm × 400 mm rectangular plan on the first floor carried by nine columns with a diameter of 10 mm, and 400 mm × 200 mm triangular plan on the second floor carried by three columns with a diameter of 8 mm. Two levels of damage were applied and the vibration records are analysed by Artemis software [36].

1.3 Objectives and new findings expected

As indicated, this study was performed on a typical residential building in the Kadıköy District of Istanbul. This building as a full-scale test specimen was subjected to different levels of damage and its dynamic behaviours was monitored by conducting AVSs. In addition, the structural behaviours were interpreted using FE numerical models. The experimentally and numerically obtained dominant frequencies and mode shapes were used to monitor the effects of the structural damages including column loss. Because of the

dynamic nature of the building, the location of the damage played an important role in damage detection. Furthermore, the column losses caused the formation of new vertical dynamic modes in the building and affected the other modes. The performed full-scale experimental study is significant for the structural health monitoring of such buildings, since it presents the dynamic properties of the undamaged and damaged forms of a real building. The extracted dominant frequencies and mode shapes were evaluated with the asymmetric structural plan of the building and the experienced damage. It was pointed out that, when the location of the damage falls in the active part of the mode shape, the change in the frequency of the mode is apparent. Moreover, the damage response of the building can be a leading finding for those dealing with the future of partially damaged buildings. As a result of the sustained damage, the quantified amount of frequency change gives a sign to assess how the structural behaviour was worsened. Secondly, the column loss scenarios specifically propound the newly developed mode. The decision of repair, strengthen, retrofit, or demolish for a partially damaged building will benefit from the findings of this study. Before giving the details of the measurement, the building and the applied damages are introduced in the next section.

## 2 Studied building and its damaged phases

A six-storey RC building is located in the Kadıköy District of Istanbul and its original form was altered by demolishing all infill walls on its ground floor in a previous study [7]. There were three independent flats on each floor which made the building a plan-asymmetric one. Its structural system contains column–beam frames with two-way beam-supported slabs with a 12 cm thickness. Column dimensions in the plan vary between 25 and 90 cm and through the height of the building they have been reduced two times. The size of the beams shows great variation. For the perimeter beams width–height dimensions were measured as 20–50 cm, while the interior beams were constructed with 15–70 cm and 20–70 cm dimensions. The type of foundation is a combination of single and continuous footings connected by link beams. The storey height is measured as 2.9 m for ground and ordinary floors, whilst it is 2.50 m on the basement floor. The studied building was symmetrically located on the site with its twin. There was no connection between them.

For the concrete quality of the building, 18 cores were extracted from its columns. Test results gave the average compressive strength of 15.2 MPa with a standard deviation of 3.2 MPa. Reinforcement details were also searched, and it was seen that S220 steel grade (characteristic yielding stress of 220 MPa was used in the structural elements). The infill walls of the building were constructed with horizontally tiled bricks and cement mortar. Their thickness was measured as 20 cm for the exterior walls and 10 cm for the interior walls. The basement floor of the building was surrounded by masonry infill walls with 50 cm thickness to prevent humidity and other effects that come from the soil. Figure 1 shows the studied building with its twin on its right-hand side, while Fig. 2 shows the structural system of the building on the basement, ground, and ordinary floors with the accelerometer locations and used terminology in the study.

The studied building was analysed for its seismic performance according to the code, LTADR [5], and because of its inadequate seismic performance, it was decided to be demolished. This situation gave an opportunity of performing destructive tests. A three-step cumulative damage consequence was planned in the building. For the post-earthquake evaluation of reinforced concrete buildings, different damage categorizations can be found in the literature. FEMA 306 [37] classifies the damage in the structural components as (i) insignificant—damage is ineffective in the structural properties, (ii) slight—damage has a small effect on the structural properties, (iii) moderate—damage has an intermediate effect on the structural properties, (iv) heavy—damage has a major effect on the structural properties, and replacement or enhancement of the damaged component may be required, (v) extreme—damage reduces the structural performance, and replacement or enhancement of the damaged component is required. Another guideline was introduced by Maeda et al. [38] and is in use for post-earthquake damage evaluation of RC buildings in Japan. This document also categorizes the existing damages in RC members in five classes as (i) slight—crack width is less than 0.2 mm, (ii) minor—crack width is less than 1 mm, (iii) moderate—crack width is around 2 mm and there is spalling of cover concrete, (iv) severe—crack width is more than 2 mm and reinforcements are exposed, and (v) collapse—there is buckling of reinforcement bars, crushing of concrete and vertical deformation of columns. In this study, the first damage covers the clear cover loss and thin cracks on structural members. This damage meets the definition of moderate damage in the classification of the aforementioned references [37, 38]. The second and third levels, respectively, cover the complete loss of columns which is the most severe damage type and is classified as extreme damage in reference [37] and collapse damage in reference [38]. In this regard, three successive damage levels as defined by damaging three columns and one beam on the ground floor of the building as illustrated in Fig. 3. The first damage is called moderate damage (MD), while the second and third damage levels were named heavy damage-I (HD-I) and heavy damage-II (HD-II), respectively.

Fig. 1 Studied building with its twin on the right-hand side
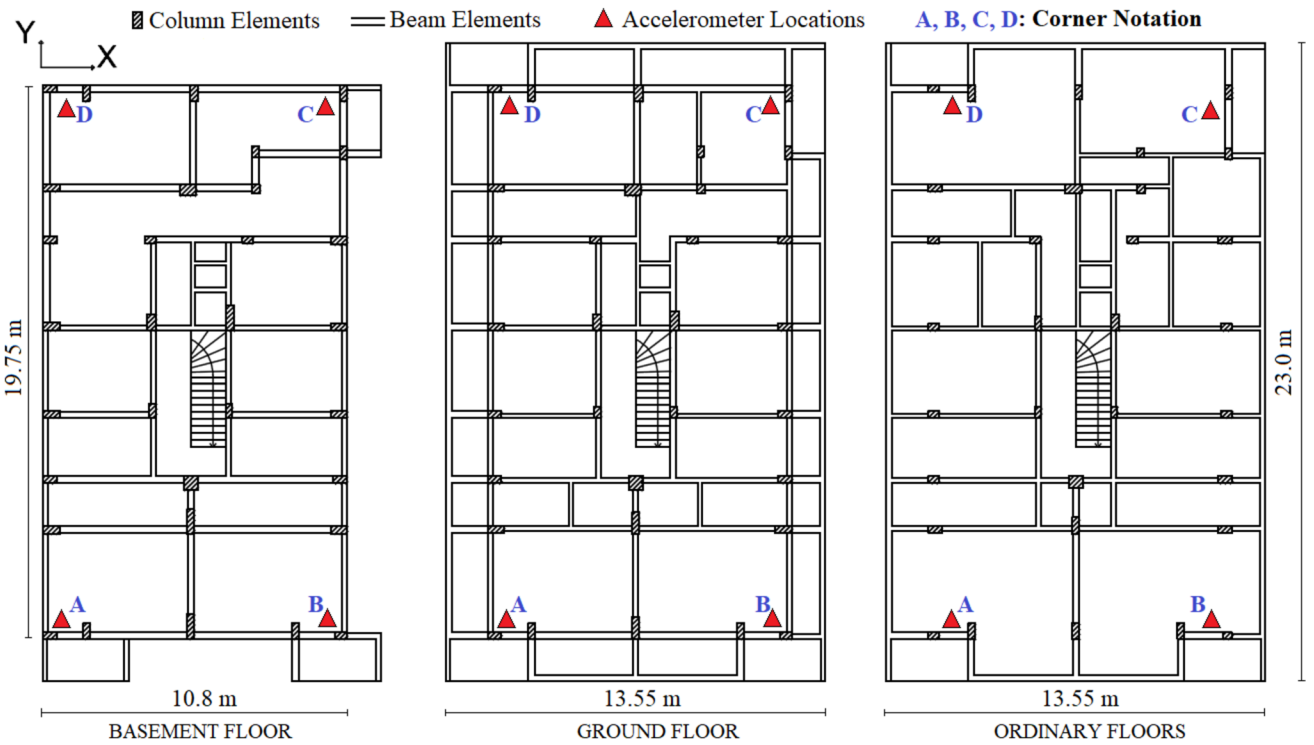
Fig. 2 The structural system of the tested building with the terminology used in the study
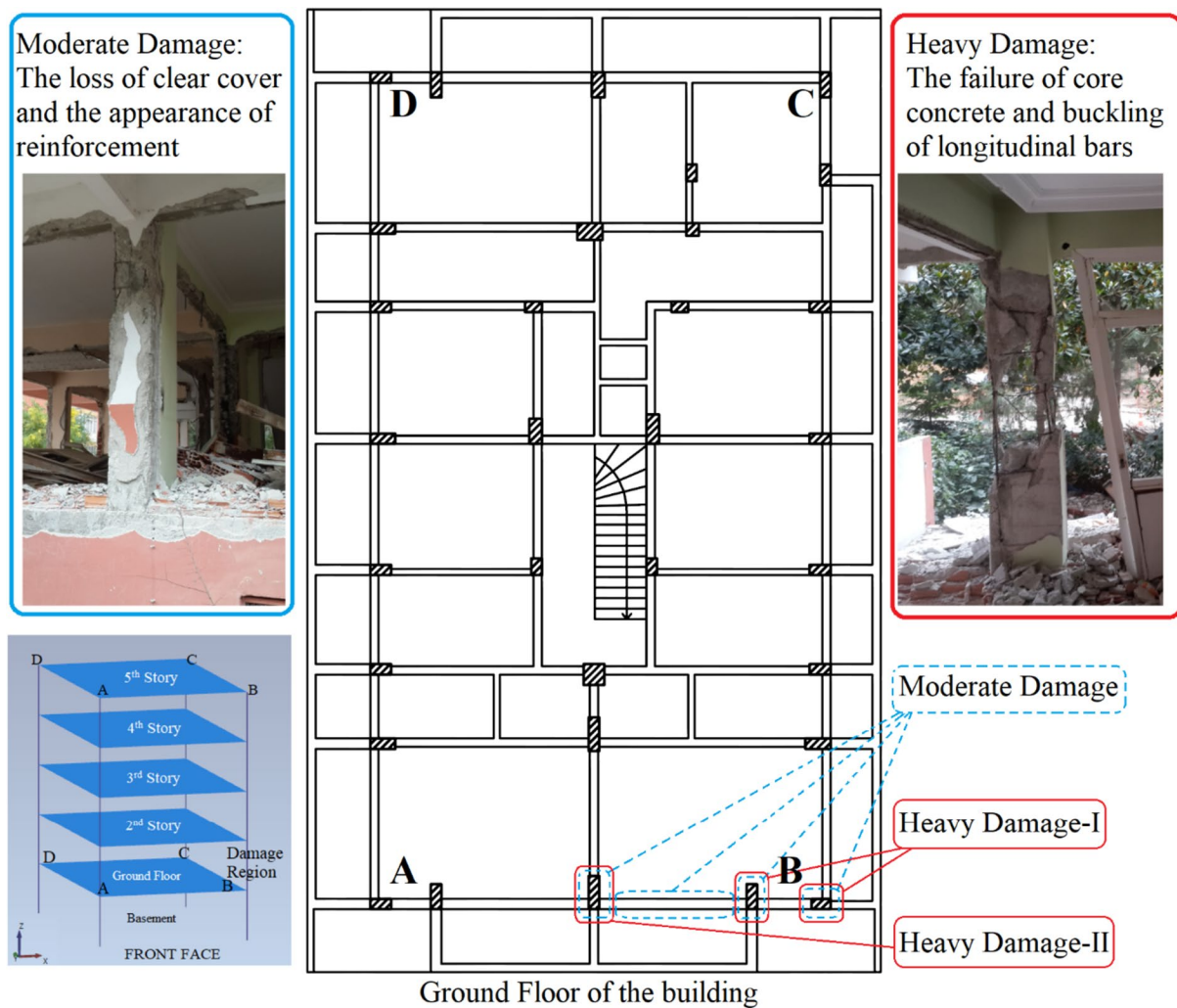
Fig. 3 Defined damage levels and their locations on the ground floor of the building and AVS model

Besides, the locations of these damages are illustrated in the model geometry formed in AVS.

3 Ambient vibration survey for the undamaged and damaged phases of the building

Ambient vibration surveys were applied to the undamaged and the damaged phases of the building. The accelerations were recorded with five Acebox force balance accelerometers [39], with three sensors oriented along with the two orthogonal horizontal directions and the vertical direction. The linear acceleration range of these sensors is $\pm 2g$, and the noise floor is less than 20 ng/$\sqrt{\text{Hz}}$. The recording was undertaken at a rate of 200 samples per second. For recordings in the two horizontal directions, the accelerometers were oriented along with the X and Y directions of

the building (see Fig. 2). One accelerometer, located on the front right-hand side corner (corner B) of the fifth storey, was used as a reference sensor; the other four sensors were located over the other stories. Six sets of measurements were recorded, each for a duration of 20 min. Figure 4 shows the locations of the acceleration measurements. The building has a closed roof system, so no measurements could be taken at the roof level.

The literature on the algorithms processing the vibration records is vast to present, but can be divided into two categories as time domain and frequency domain analyses [40, 41]. Stochastic subspace identification (SSI) and enhanced frequency domain decomposition (EFDD) methods are the most frequently used techniques for output only modal identification studies in the time and frequency domains, respectively. Few studies have employed both to identify the dynamics of complicated structures and concluded that they yield similar results [42–44]. The
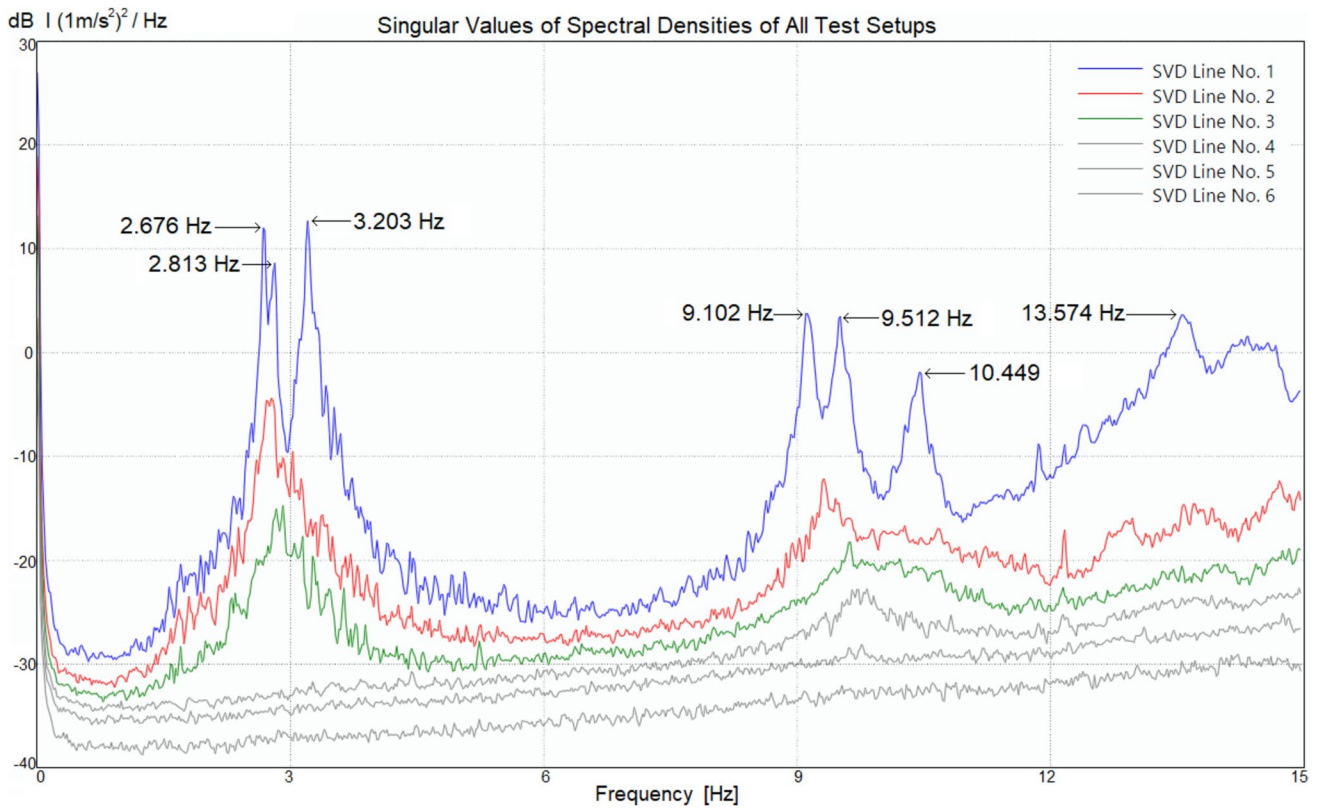
Fig. 4 Singular values of spectral density for the AVS of the undamaged building

well-known enhanced frequency domain decomposition method was used in this work, employing Artemis modal analysis software [36]. In the EFDD technique, the relationship between the unknown input and the measured responses can be expressed as:

$$\left[G_{yy}(j\omega) \right] = \left[H(j\omega) \right]^* \left[G_{xx}(j\omega) \right] \left[H(j\omega) \right]^T, \tag{1}$$

where $\left[G_{xx}(j\omega) \right]$ is the power spectral density (PSD) matrix of the input, $\left[G_{yy}(j\omega) \right]$ is the PSD matrix of the responses, $\left[H(j\omega) \right]$ is the frequency response function (FRF) matrix, * and superscript T denote the complex conjugate and transpose, respectively. By noting that the input is white noise, the PSD matrices of output signals can be diagonalized by singular value decomposition as shown in Eq. 2 after a set of mathematical operations and transformations.

$$G_{yy}\left(j\omega_i \right) = U_i S_i U_i^T, \tag{2}$$

where the matrix $U_i = [u_{i1}, u_{i2}, \dots u_{im}]$ is a unitary matrix holding the singular vectors u_{ij}, and s_{ij} is a diagonal matrix holding the scalar singular values. The first singular vector u_{ij} is an estimation of the mode shape. PSD function is identified around the peak by comparing the mode shape estimation u_{ij} with the singular vectors for the frequency lines around the peak [41]. The spectral resolution was used as 1024 for spectral density estimation. Modal identification was performed between 0 and 20 Hz, which was adequate for the identification of the building.

Although the dynamic properties are inherent properties that are theoretically dependent on the mass and stiffness parameters of the structures, recent studies proved their dependency on the environmental effects, such as traffic, wind, humidity, solar radiation, and, most importantly, temperature [45–49]. Aras [49] concluded that a 28 °C temperature drop caused more than 4% increase in the first dominant frequency of an RC pedestrian bridge and the return in temperature also returned the dominant frequency to its initial value. Secondly, according to the result of a set of dynamic testing under ambient and forced conditions, it was proven that the magnitudes of the vibrations can alter the obtained dominant frequencies of the buildings [50]. Therefore, to perform a reliable assessment, the interference of these parameters must be distinguished from the damage effects. In this study, to prevent the mentioned environmental effects from masking the effects of structural damages, all measurements were gathered on two consecutive days in which daily temperatures were in the same range. Besides, during the measurement,

no additional vibrations other than the wind or low traffic stream on the street were created on the site.

In the mid-rise RC buildings, the first three dynamic modes usually govern the dynamic response of the buildings and these modes form a high amount of modal mass participation ratio. The higher modes are still important for damage detection purposes and monitoring the change in the building response. For these reasons, in this study, priority is given to the first three modes of the building, and higher modes are briefly mentioned.

3.1 AVS of the undamaged building

To determine the dominant frequencies and mode shapes of the undamaged building, acceleration records were gathered from the building and analysed with the given details above. Figure 4 shows the singular values of the spectral density of the signals taken from the building in the X, Y, and Z directions. The first six modes of the building are shown in Fig. 5. The first mode is a torsional mode formed mainly by the movement of the front face in the X direction with a dominant frequency of 2.676 Hz. In the second mode, the movement of the back face of the building forms the torsional behaviour with a frequency of 2.813 Hz. The third mode of the building is the movement of the whole building in the Y direction with a dominant frequency of 3.203 Hz. The fourth, fifth, and sixth modes of the building are the dual curvature modes of the first, second, and third

modes with dominant frequencies of 9.102 Hz, 9.512 Hz, and 10.449 Hz, respectively. The next frequency at around 13.5 Hz is also searched. It is seen that this mode is formed by the vertical movement of corner A on the fifth storey. Since the accelerometers have been located on the slabs, their out-of-plane stiffness must be an effective parameter. However, these modes are not important for representing the general dynamic behaviour of the building.

The obtained dynamic properties revealed the important structural features of the building. Note that the structural system of the building is not a symmetrical one. Besides, on each floor of the building, there are three independent flats which make the infill wall orientations asymmetric as well. Hence, the first two modes of the building are torsion coupled. Secondly, the formation of soft-storey mechanism on the ground floor was noted for all modes. The lack of infill walls on the ground floor of the building is the main reason for the soft storey irregularity. Based on the definition of the torsional and soft-storey irregularities in IBC [51], ASCE-SEI 7-10 [52] and TBEC [4], Aras et al. [7] conducted detailed analyses with the extracted mode shapes of the building. Therefore, more detailed information can be found in Aras et al. [7].

Figure 6 shows the modal assurance criterion (MAC), which was used to assess the similarity of the two calculated modes. The MAC is defined in Eq. 3, where T stands for transpose, and $\{\phi_i\}$ and $\{\phi_j\}$ are the ith and jth mode shape vectors of the structure, respectively [53]. An MAC
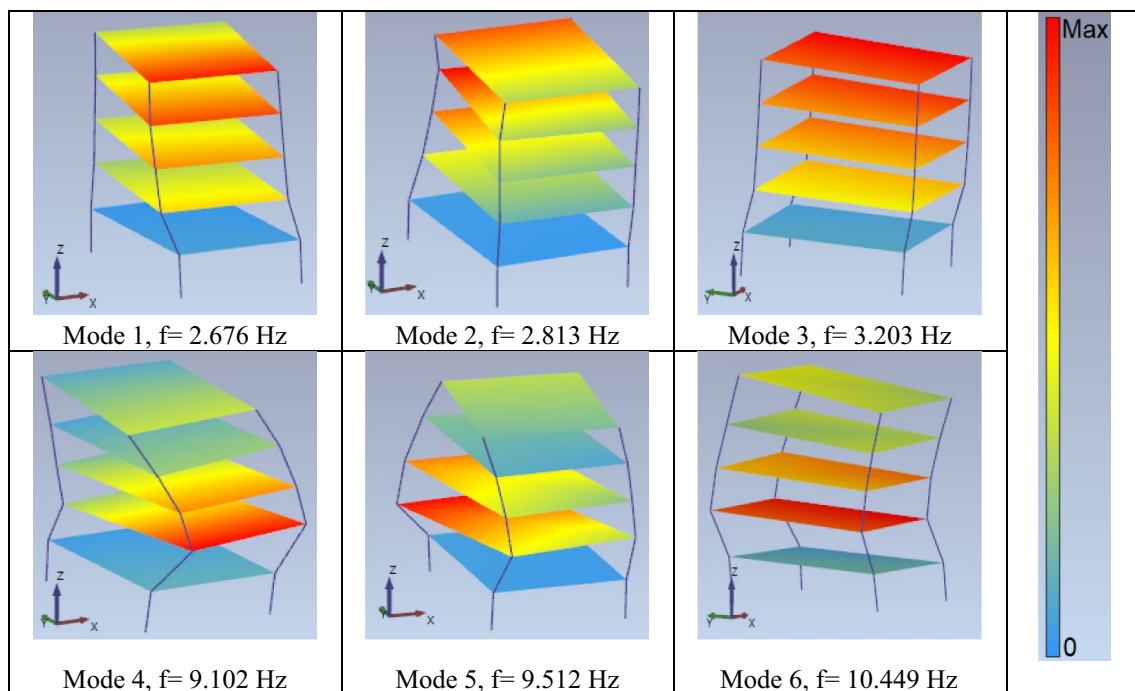

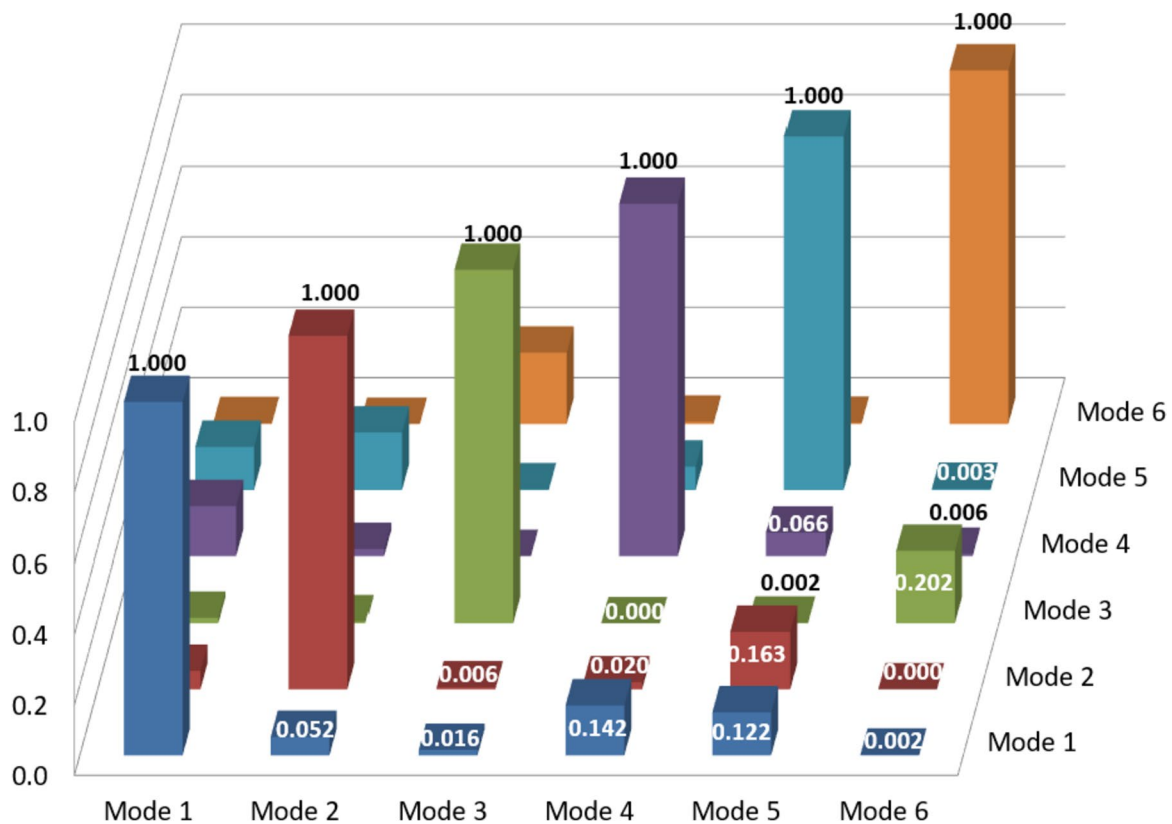**Fig. 5** Mode shapes and dominant frequencies of the building

Fig. 6 MAC values for the estimated first six modes

near zero indicates that these modes are well separated; if the MAC is near unity, the modes are similar to each other. Thus, the obtained MAC values between two different modes should be close to zero for mode separation. The MAC values obtained in this work proved the consistency of the estimated mode shapes.

$$\text{MAC} = \frac{\left|\{\phi_i\}^{\text{T}}\{\phi_j\}\right|^2}{\{\phi_i\}^T\{\phi_i\}\{\phi_j\}^T\{\phi_j\}}. \tag{3}$$

3.2 AVS for the MD phase of the building

In this stage, two corner columns located on the right front (corner *B*), the column on the middle-front region of the building, and the beam connecting the middle-front column to the left-front corner columns were damaged by a construction-demolishing machine. Until the peel-off of the clear cover concrete, vibrational impacts were applied. Locally in some regions, longitudinal bars accidentally separated from the core, but no cracks developed in the core concrete of the columns. Besides, the beam experienced more damage than intended due to the difficulty of the application

of the impacts caused by the overhangs. Figure 7 shows the damaged members.

AVS was applied to the building with the same principles explained before. The first three dominant frequencies of the building were determined as 2.656, 2.793, and 3.184 Hz (Fig. 8). The general mode shape definitions of the building remained the same as those determined for the undamaged building. Concerning the previous phase, a slight decrease in the dominant frequencies was noted. The same conclusion is valid for the higher modes except for the fifth mode.

3.3 AVS for HD-I phase of the building

In this phase, two corner columns were heavily damaged. They were razed, and Fig. 9 shows the damaged elements in this phase. Figure 10 shows the singular values of spectral density illustration. The first three dominant frequencies of the building were determined as 2.578, 2.793, and 3.164 Hz, proving that the second mode frequency did not change, but the frequencies of other modes decreased slightly. Mode shapes visually remained the same as those for the undamaged building. One distinct difference concerning the previous case was the dominant frequency seen at 12.168 Hz. The mode shape evaluation pointed out that this mode did not

Fig. 7 Three damaged columns and one beam for moderate damage (MD)
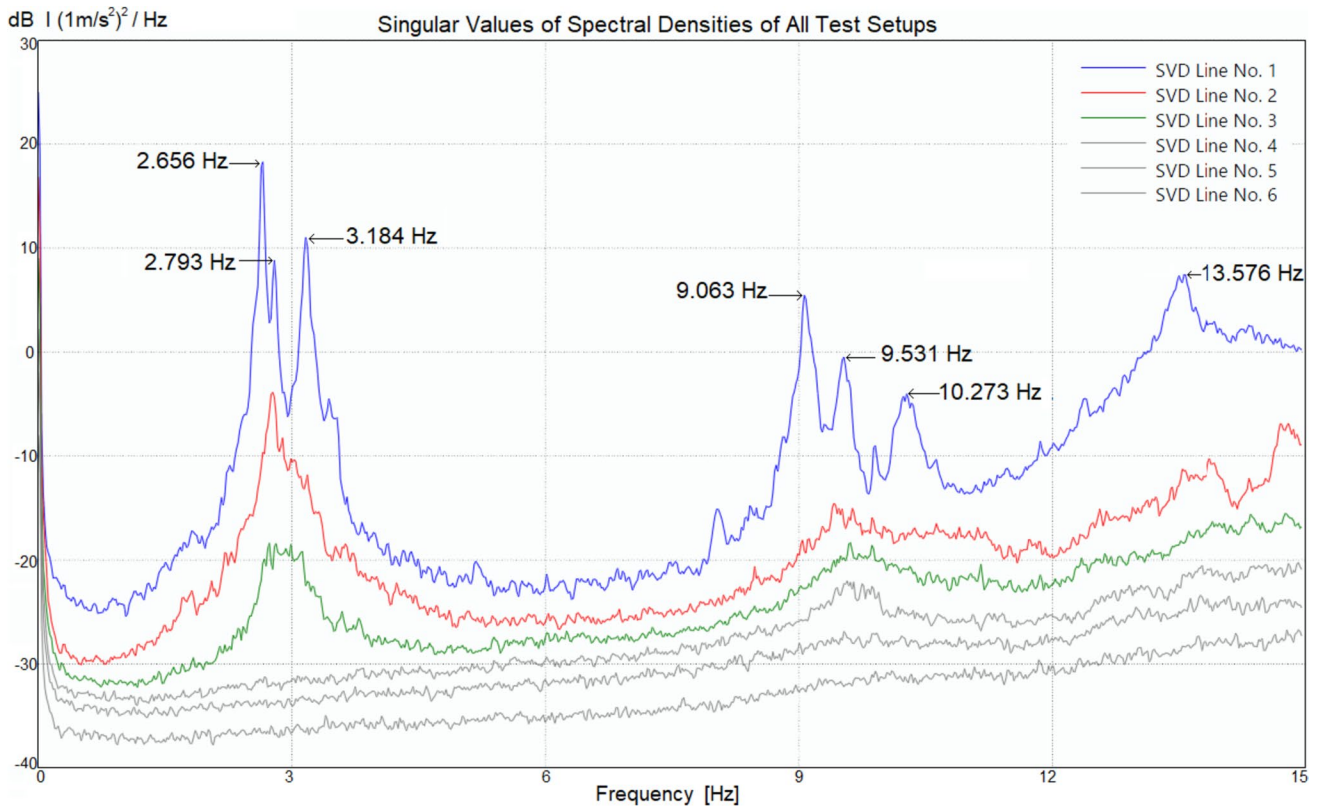
Fig. 8 Singular values of spectral density for the MD phase of the building

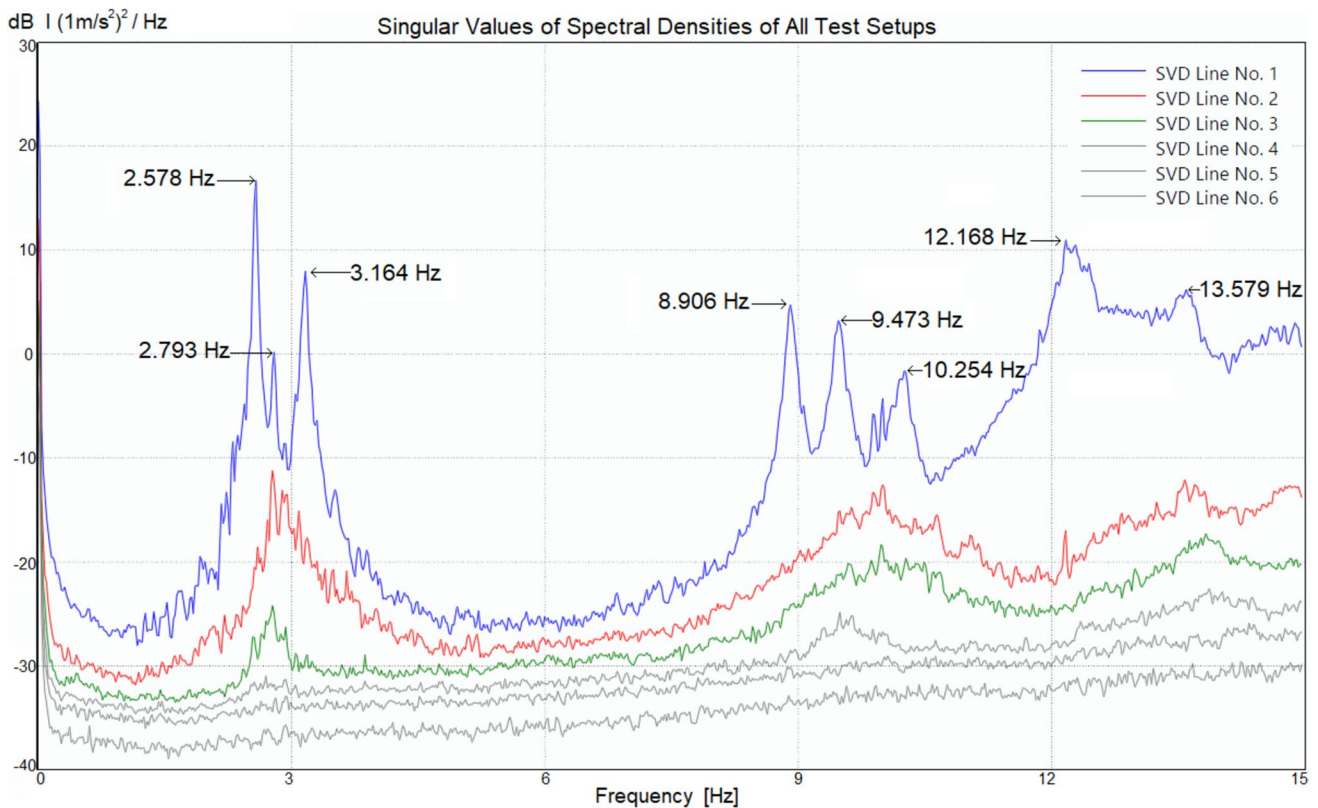**Fig. 9** Two heavily damaged corner columns for HD-I

Fig. 10 Singular values of spectral density for HD-I

exist for the previous cases and it was formed by the vertical movement of corner *B*, where column damages existed on the ground floor. In other words, the given damage created a vertical mode.

3.4 AVS for HD-II phase of the building

The moderately damaged column was heavily damaged in this phase. Figure 11 shows the damaged elements and Fig. 12 shows the singular values of spectral density illustration for the HD-II phase of the building. The dominant frequency of the second mode did not change again, but those

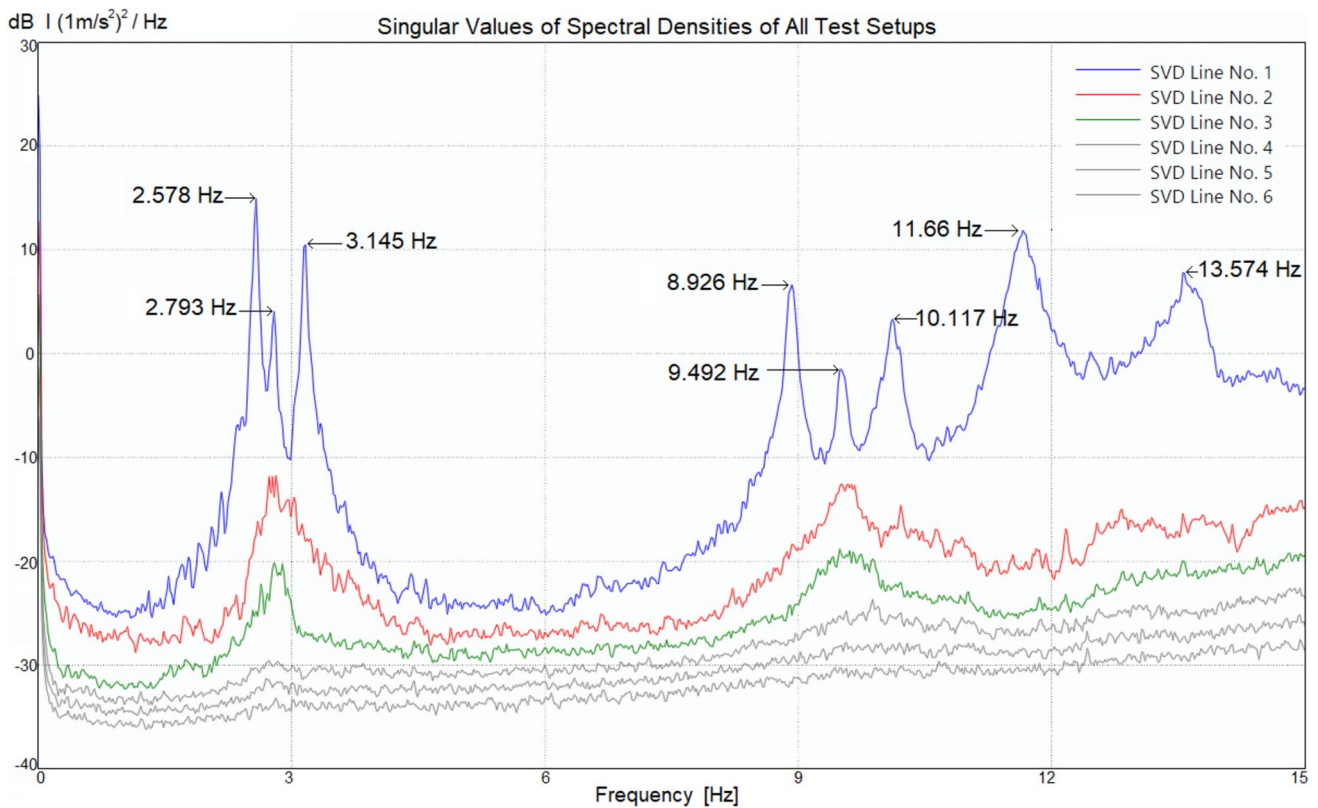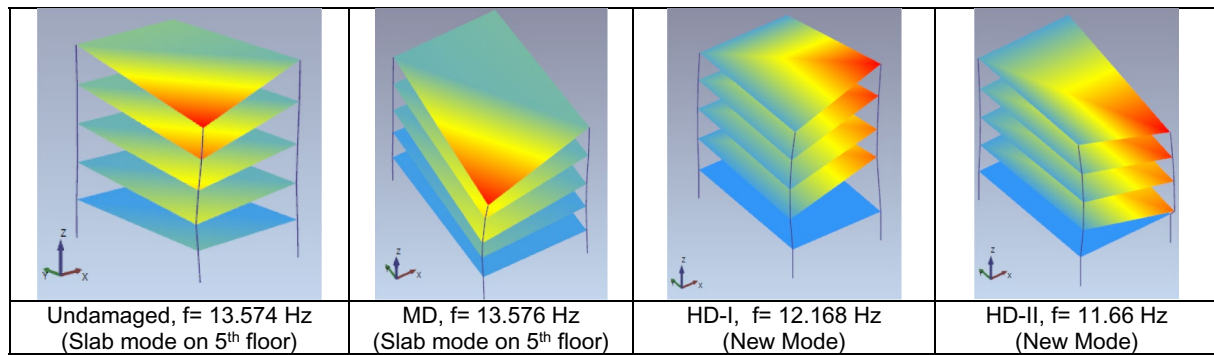**Fig. 11** Heavily damaged three columns for HD-II

Fig. 12 Singular values of spectral density for HD-II

of other modes decreased slightly. Mode shapes remained the same as those for the original building. The vertical mode induced by the heavy damages had a dominant frequency of 11.66 Hz.

Figure 13 has been prepared to evaluate high-frequency modes and present the formation of a new dynamic mode for the HD-1 and HD-2 stages. For the undamaged and MD phases of the building, the seventh dominant frequency is seen at around 13.57 Hz and represents the mode shape

| Undamaged, f= 13.574 Hz (Slab mode on 5th floor) | MD, f= 13.576 Hz (Slab mode on 5th floor) | HD-I, f= 12.168 Hz (New Mode) | HD-II, f= 11.66 Hz (New Mode) |

**Fig. 13** Seventh mode of the building for its different phases

Table 1 The modal frequencies of the building through the damage states and their difference from the undamaged phase determined with AVS

Mode number	Frequency of the building for its different phases, Hz				Variation in frequency, %		
	Undamaged	MD	HD-I	HD-II	MD	HD-I	HD-2
Mode 1	2.676	2.656	2.578	2.578	− 0.75	− 3.66	− 3.66
Mode 2	2.813	2.793	2.793	2.793	− 0.71	− 0.71	− 0.71
Mode 3	3.203	3.184	3.164	3.145	− 0.59	− 1.22	− 1.81
Mode 4	9.102	9.063	8.906	8.926	− 0.43	− 2.15	− 1.93
Mode 5	9.512	9.531	9.473	9.492	0.20	− 0.41	− 0.21
Mode 6	10.449	10.273	10.254	10.117	− 1.68	− 1.87	− 3.18
Mode 7	13.574	13.576	13.579	13.574	− 0.57	0.04	0.00
New mode	–	–	12.168	11.66	–	–	− 4.17

formed by mainly vertical movement of corner A on the fifth floor. At around the same frequency, this mode also exists in HD-I and HD-II stages and is related to the stiffness of the slab on which the accelerometer is located. Therefore, this partial mode does not simulate the global dynamic response of the building. However, for HD-I and HD-II the seventh dominant frequency was identified at 12.168 Hz and 11.66 Hz, respectively. The mode shape for both was the vertical movement of corner *B*, where column losses were experienced on the ground floor. In that respect, these modes are new modes developed by the sustained damage. One particular conclusion here is that damage not only changes modal frequencies, but also adds a new mode consistently observed in both HD-I and HD-II cases.

4 Effects of damages on the frequencies of the building

The dynamic properties of structures are altered by the occurrence of damage, since the rigidity of the members forms the rigidity of the structure. The dominant frequencies are the most basic dynamic parameters that point to the existence of damage. The results of the AVSs for the undamaged and damaged phases of the building are summarized in Table 1. Figure 14 illustrates the variation of dominant
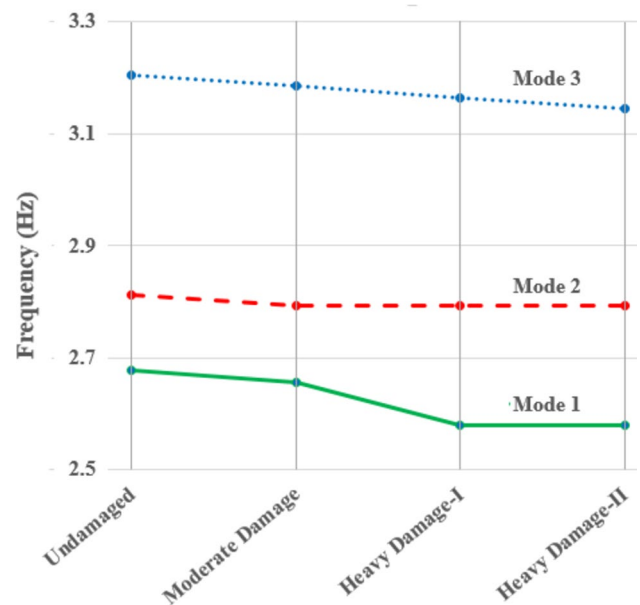
Fig. 14 The first three modal frequencies of the building through the sustained damage levels

frequencies for the main modes, while Fig. 15 does it for the higher modes additionally showing the formation of a new mode for the heavily damaged building. To evaluate the
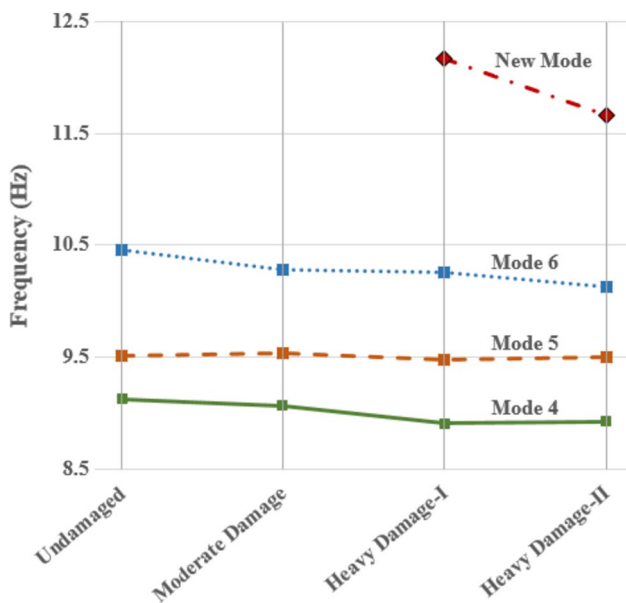
Fig. 15 The variation of the modal frequencies of higher modes through the sustained damage levels

amount of the change in the frequencies as a result of the experienced damage, the coefficient, ε_i, is calculated with Eq. 4, where f_i^D is the ith mode frequency of the damaged building and f_i^U is the ith mode frequency of the undamaged building.

$$\varepsilon_i = \frac{f_i^D - f_i^U}{f_i^U}. \tag{4}$$

The first mode frequency of the building decreased with the experienced damage. Unexpectedly, the decreases for the HD-I and HD-II phases are the same. The obtained second mode frequencies of the building are the same for all damage stages and it is 0.71% less than that of the undamaged building. The third mode frequency decreases with the increase in the severity of the damage. The complete loss of three columns (out of 32) on the ground floor caused a decrease of less than 4% in the dominant frequency of the first mode. Such a small amount of decrease can be regarded as an insignificant change to worsen the dynamic behaviour of the building. For the decision-makers working on the assessment of partially damaged buildings, the result can favour the repair or retrofit of them.

The building under investigation is a plan-asymmetric building with asymmetric damage and the dynamic modes of the building are torsion-coupled modes, especially for the first and second modes. It is seen that the modes containing the movement of the damaged parts in their shape are affected by the damage significantly. The first mode of the building was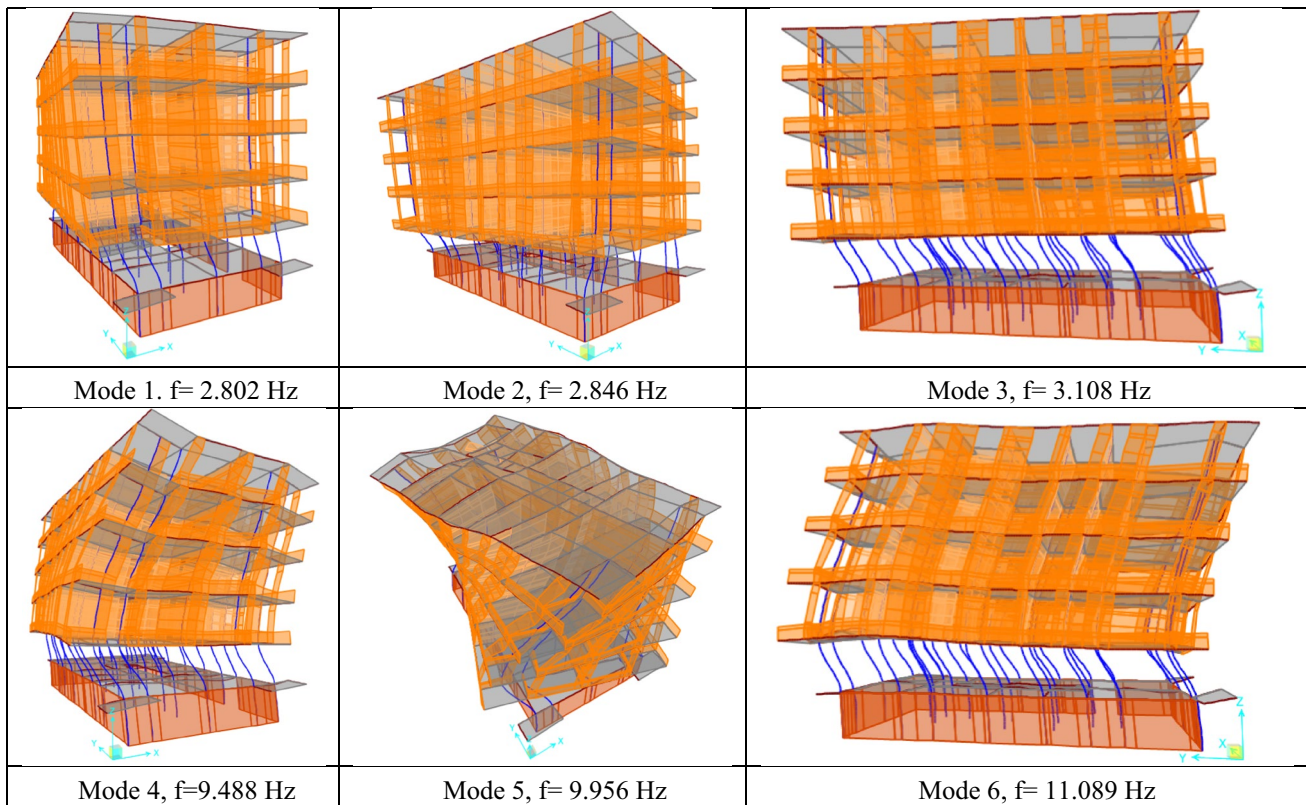 defined as the movement of the front face of the building in the *X* direction and the location of the damage remains in the most active part of the mode. For this reason, the first mode frequency was affected by the damage considerably. For the second mode, the damage location was out of the active part of the mode shape, which was defined as the movement of the back face of the building in the *X* direction. Therefore, the sustained damage may not alter the dominant frequency of the second mode significantly. The third mode was the movement of the building in the *Y* direction and the damage location was within the active part. Hence, the sustained damage affected its frequency.

The loss of two corner columns in the HD-I phase makes the corner *B* unsupported in the vertical direction. For this reason, a new mode, which did not exist for the undamaged and moderately damaged building, was created with a dominant frequency of 12.168 Hz. When the building lost one more column, the dominant frequency of the new mode decreased to 11.66 Hz. In this study, numerical analyses were also employed for the validation of the experimental results.

5 Numerical investigation for the undamaged and damaged phases of the building

5.1 Numerical model and dynamic properties of undamaged buildings

For the construction of the most suitable numerical model, exhibiting the dynamic properties extracted from AVS, two extensive research were completed by Aras et al. [6, 7]. In the first study, Aras et al. [6] constructed the numerical model of the building in SAP2000 by using frame elements for columns and beams and shell elements for slabs. The authors favoured the use of shell elements for infill walls to visualize the dynamic behaviour of RC buildings under low-level vibration. In the second study, Aras et al. [7] analysed two forms of buildings, namely, (i) the original building which had masonry infill walls on each floor and (ii) the altered building whose ground floor's masonry infill walls had been demolished. The authors employed an interactive model tuning procedure and obtained the most suitable numerical model representing the dynamic behaviour of both phases. As the results of the procedure, the modulus of elasticity of the concrete and infill walls were determined as 37,000 MPa and 2700 MPa, respectively. The numerical model representing the undamaged building is the one for the altered form validated by Aras et al. [7]. Its dynamic properties derived from eigenvalue analysis are shown in Fig. 16 and Table 2. It is seen that the first six modes of the numerical model fit those obtained experimentally. The higher modes are composed of partial movement of slabs

Mode 1. f= 2.802 Hz	Mode 2, f= 2.846 Hz	Mode 3, f= 3.108 Hz
Mode 4, f=9.488 Hz	Mode 5, f= 9.956 Hz	Mode 6, f= 11.089 Hz

Fig. 16 The mode shapes and dominant frequencies of the undamaged building determined by FEA

Table 2 Dynamic properties of the tuned numerical model

Mode	Period	Frequency	Participation ratio		Total participation ratio	
	s	Hz	X dir	Y dir	X dir	Y dir
1	0.357	2.802	0.274	0.022	0.274	0.022
2	0.351	2.846	0.575	0.026	0.849	0.048
3	0.322	3.108	0.002	0.812	0.851	0.860
4	0.105	9.488	0.042	0.000	0.893	0.860
5	0.100	9.956	0.006	0.001	0.899	0.861
6	0.090	11.089	0.000	0.028	0.899	0.889

and infill walls which cannot be detected experimentally. The first three modal frequencies are 2.802 Hz, 2.846 Hz, and 3.108 Hz. The difference in the dominant frequencies of AVS and FEA, ε_i, was calculated with Eq. 5 and computed as 4.7%, 1.2%, and -3%.

$$\varepsilon_i = \frac{F_i^{FEA} - F_i^{AVS}}{F_i^{AVS}}. \tag{5}$$

Modal assurance criterion (MAC) values [53] were also calculated to evaluate the similarity between the experimentally and numerically obtained mode shapes by Eq. 6, where Φ_i^{FEA} is the numerically obtained ith modal vector, and Φ_i^{AVS} is the experimentally obtained ith modal vector. If the MAC calculated for two modes is near zero, this shows that these modes are well separated. If it is near unity, the modes are similar to each other. Mode shape vectors were arranged to include the modal displacement of four corners of each storey in the building. The modal displacements along the X direction were used for the assessment of the first two modes, since these modes were mainly in the X direction. Because of the same reason, the modal displacements along the Y direction were used in the third mode.

Table 3 The modal frequencies of the building through the damage states and their difference from the undamaged phase determined with FEA

Mode number	Frequency of the building for its different phases, Hz				Variation in frequency, %		
	Undamaged	MD	HD-I	HD-II	MD	HD-I	HD-2
Mode 1	2.802	2.710	2.620	2.592	− 3.27	− 6.49	− 7.50
Mode 2	2.846	2.845	2.843	2.839	− 0.05	− 0.13	− 0.26
Mode 3	3.108	3.067	3.025	2.915	− 1.33	− 2.69	− 6.24
Mode 4	9.488	9.398	9.604	9.414	− 0.95	1.22	− 0.78
Mode 5	9.956	9.925	9.913	9.909	− 0.30	− 0.43	− 0.47
Mode 6	11.089	10.998	11.295	11.104	− 0.82	1.86	0.14
New mode	–	–	8.482	7.945	–	–	− 6.33
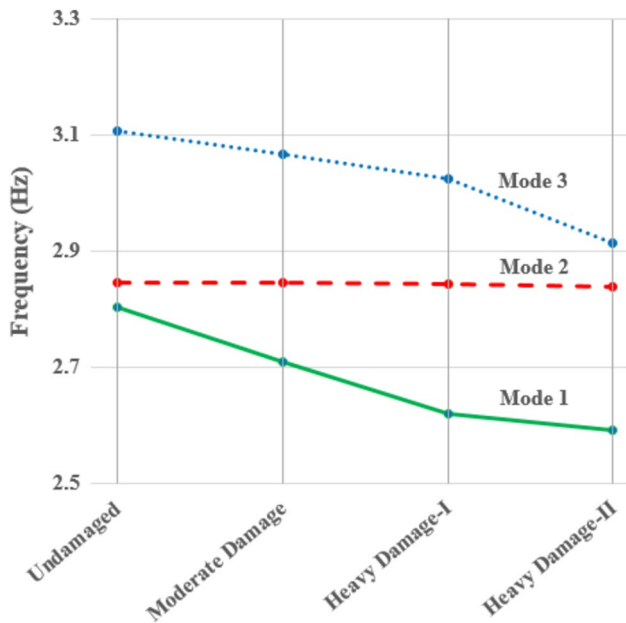
Fig. 17 The variation of modal frequencies through the sustained damage levels determined by FEA

Fig. 18 The variation of modal frequencies of higher modes through the sustained damage levels determined by FEA

$$\mathrm{MAC} = \frac{\left[\left(\Phi_i^{\mathrm{FEA}}\right)^{\mathrm{T}}\left(\Phi_i^{\mathrm{AVS}}\right)\right]^2}{\left(\Phi_i^{\mathrm{FEA}}\right)^{\mathrm{T}}\left(\Phi_i^{\mathrm{FEA}}\right)\left(\Phi_i^{\mathrm{AVS}}\right)^{\mathrm{T}}\left(\Phi_i^{\mathrm{AVS}}\right)}. \tag{6}$$

For the undamaged building, MAC values between the experimental and numerically obtained first, second, and third modes were computed as 0.98, 0.97, and 0.96, respectively. These values prove that the experimentally and numerically obtained modes were in good agreement for the undamaged building.

5.2 Dynamic properties of the building for MD, HD-I, and HD-II damage states

The numerical model of the undamaged building was revised to obtain that of the building in the MD phase. Since the MD accounts for clear cover lost in three columns and
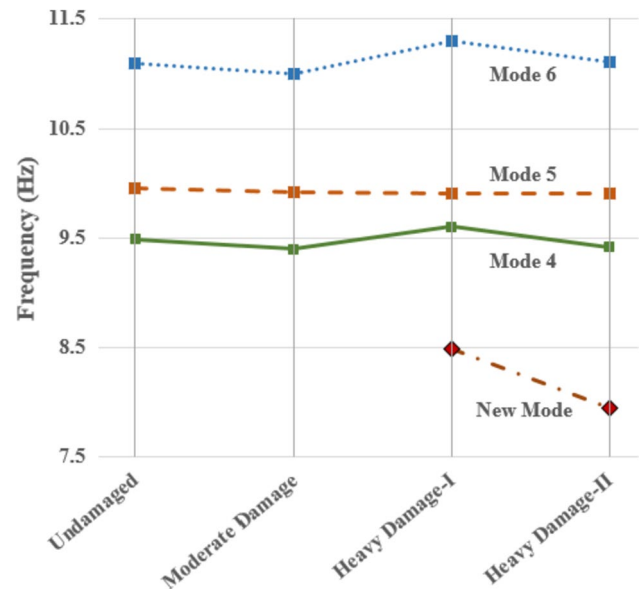
one beam, the cross-sectional dimensions of these elements were reduced by 6 cm, due to 3 cm clear cover on each side. Eigenvalue analysis, performed with this model, gave the dynamic properties of the building in the MD phase. Because of the demolished columns in the HD-I and HD-II stages, the numerical models of the building in these stages were obtained by removing the specified columns from the numerical model constructed for the MD phase of the building. Dynamic analyses were repeated for each phase of the building. The obtained dynamic properties for the four phases of the building are summarized in Table 3. Figures 17 and 18 illustrate the variation of the first three dominant frequencies and higher frequencies, respectively.

It is seen that, for the building in MD, there is a slight decrease in the dominant frequencies and the mode shapes remained the same as those determined for the undamaged building. For HD-I, a slight frequency decrease with respect to MD was observed in the respective modal frequencies, except those of the fourth and sixth modes. Additionally, a

new mode as the vertical movement of corner *B*, where column loss exists, appeared with a frequency of 8.482 Hz. The appearance of this mode also affected the mode shapes of the other higher modes. The fourth, fifth, and sixth modes of the heavily damaged building are not the same as those of the undamaged and moderately damaged building. The dynamic analysis performed for the building in HD-II indicated slight decreases concerning the HD-I phase.

According to Table 3, the sustained damage generally decreased the frequency of the modes. It is seen that the first and third modes are the mostly affected mode by the damage, while the second mode is not affected much. The same interpretation was valid for the experimental analysis as well. It is also noted that, the fourth and sixth mode frequencies were slightly increased in HD-I. A similar frequency increase had been detected in the fifth mode of the building in MD. These small amounts of frequency increases in the higher modes may be the results of changes in the global stiffness matrix.

The numerical results also pointed that the column loss caused a new mode to develop as the vertical movement of the damaged corners through the height of the building. This new developed mode is the indication of a global change in the stiffness of the building and may cause two unexpected frequency increases in the fourth and sixth mode of the building as a result of heavy damage. It should be noted that the dominant frequency of the new mode is less than that of the fourth mode, contrary to the experimental results.

The comparison of the damage coefficients computed for each mode and each damage level between the AVS and FEA proves that numerical analysis signifies the effect of damage. For the first three modes, the relation between the severity of the damage and the decrease in the frequencies was confirmed, but for the higher modes the sustained damage caused even some increases in the frequencies. Like the experimental results, numerical analyses also showed that when the active part in a mode is damaged, the frequency of the mode decreases. However when a stationary portion in a mode is damaged, the frequency of the mode is not affected significantly. That is why the damaged front, right-hand side of the ground floor caused a significant decrease in the modal frequency of first mode of the building, which was determined as the lateral movement of the front face of the building. Similarly, the damaged front, right-hand side of the ground floor caused only a small amount of decrease in the modal frequency of the second mode in which the front face of the building did not move.

6 Conclusions

In this study, an existing reinforced concrete building with an asymmetric structural plan and soft storey irregularity was used as a test specimen. The dynamic properties of the undamaged phase of the building were determined by AVS. Later on, three progressive structural damage levels were applied to three columns and one beam, located on the front, left-hand side part of its ground floor, and its dynamic properties were obtained for each level.

Confirming the asymmetric plan geometry of the building, the first three mode shapes were obtained as torsion-coupled modes. The first mode of the building was the movement of the front face of the building in the *X* direction, while the second mode was the movement of the back face of the building in the *X* direction. The third mode is the movement of the building in the *Y* direction. The fourth, fifth, and sixth modes of the building were the double curvature forms of the first, second, and third modes. Hence, the findings of the study are important for the structural health-monitoring assessment of the non-symmetric buildings that experienced non-symmetric damages.

Three-level progressive damages showed different degrees of effectiveness in the dominant frequencies of the modes. As a result of the most severe damage, the amount of change in the dominant frequency was 3.66% for the first mode, 1.88% for the third mode, and 0.71% for the second mode. It should be noted that the location of the damage was on the active portion of the building in the first mode, which was the movement of the front face of the building in the *X* direction. The third mode was the movement of the building in the *Y* direction. Finally, in the second mode, the front face was not active. It can be concluded that when the location of the damage falls in the active part of the mode shape, the change in the frequency of the mode is apparent.

The visual inspection of the mode shapes of the original and the damaged phases of the building showed that they remained the same. On the other hand, after experiencing column loss, a new mode developed as the vertical movement of the corner where the columns were razed. The dominant frequency of the new mode was determined as 12.168 Hz, which was more than the frequency of the sixth mode of the building in HD-I and decreased by 11.66 Hz in HD-II. These new structural modes observed after the damage may lead to quick assessment of such buildings after earthquakes where timely objective assessment is important.

FEAs performed for the undamaged and three damaged phases of the building showed that the damage-induced decrease in the dominant frequencies of the building was more than those obtained in the experimental study. However, the finding, "when the location of the damage falls in

the active part of the mode shape, a decrease in the dominant frequency of the mode is apparent", was confirmed. The loss of columns resulted in the development of a new vertical mode, as the movement of the corner remained unsupported. The dominant frequency of this vertical mode was 8.482 in HD-I and decreased to 7.945 Hz in HD-II. In that respect, this mode is seen as the fourth mode in FEA.

The finding, "when the location of the damage falls in the active part of the mode shape, a decrease in the dominant frequency of the mode is apparent", can be used for the effective and economical sensor placement strategies in structural health-monitoring projects of torsion-dominated structures. The location and the direction of uniaxial accelerometers can be arranged according to the torsion-dominated modes to detect the damage efficiently.

It was determined that the overall collapse of the 3 out of 32 columns on the ground floor of the building caused at most a 3.66% reduction in its dominant frequencies. This amount of reduction can provide valuable information to the decision makers for the future of partially damaged RC buildings towards repair or retrofit options instead of demolition. In this condition, reconstruction of the lost elements is important for the recovery of the original structural behaviour to prevent the newly developed modes seen in this study.

Data availability As obtained after testing a real-life building within a scientific project, the obtained data will be used in further scientific studies. For this reason, the data are not available to share for the time being. However, a reasonable request to the corresponding author is always welcome.

Declarations

Conflict of interest The authors declare that they have no conflict of interest.

References

1. Kaltakci MY, Arslan MH, Korkmaz HH, Öztürk M (2007) An investigation on failed or damaged reinforced concrete structures under their own-weight in Turkey. Eng Fail Anal 14:962–969

2. Arslan MH, Korkmaz HH (2007) What is to be learned from damage and failure of reinforced concrete structures during recent earthquakes in Turkey? Eng Fail Anal 14:1–22

3. ABYYHY (2007) Afet Bölgelerinde Yapılacak Yapılar Hakkında Yönetmelik (Specification for structures to be built in disaster areas). Ministry of Environment and Urbanization, Ankara

4. TBEC (2018) Turkish building earthquake code. Ministry of Environment, Urbanization and Climate Change, Ankara

5. Turkish Republic (2012) LTADR: the law about the transformation of the areas under disaster risk. Law No: 6306, Date: 31.05.2012. Official Gazette of Turkish Republic. Ankara. http://webdosya.csb.gov.tr/db/altyapi/editordosya/6306SAYILIKANUN-degisiklikislenmissonhali.pdf

6. Aras F, Akbas T, Çeribasi S, Çatbaş FN (2021) Modelling of infill walls in reinforced concrete buildings under low-amplitude vibrations. Proc Inst Civ Eng Struct Build. https://doi.org/10.1680/jstbu.20.00310

7. Aras F, Akbas T, Çeribasi S, Çatbaş FN (2021) Full-scaled experimental and numerical investigation on the contribution of masonry infill walls into dynmaic behavior of RC buildings. Struct Control Health Monit 29:e3141

8. Sozen MA, Thornton CH, Corley WG, Mlakar PF (1998) The Oklahoma City bombing: structure and mechanisms of the Murrah building. J Perform Constr Facil 12(3):120–136

9. Kazemi-Moghaddam A, Sasani M (2015) Progressive collapse evaluation of Murrah Federal Building following sudden loss of column G20. Eng Struct 89(2015):162–171

10. Parisi F, Scalvenzi M (2020) Progressive collapse assessment of gravity-load designed European RC buildings under multi-column loss scenarios. Eng Struct 209:110001

11. El-Demerdash WE, El-Metwally SE, El-Zoughiby ME (2020) Survival of reinforced concrete flat plate system against column loss. Electron J Struct Eng 20(1):33–44

12. Hou R, Xia Y (2021) Review on the new development of vibration-based damage identification for civil engineering structures: 2010–2019. J Sound Vib 491:115741

13. Gudmundson P (1982) Eigen frequency changes of structures due to cracks, notches or other geometrical changes. J Mech Phys Solids 30(5):339–353

14. Springer WT, Lawrence KL, Lawley TJ (1988) Damage assessment based on the structural frequency response function. Exp Mech 28(1):34–37

15. Cawley P, Adams RD (1979) The location of defects in structures from measurements of natural frequencies. J Strain Anal 4(2):49–57

16. Heam G, Testa RB (1991) Modal analysis for damage detection in structures. J Struct Eng ASCE 117(10):3042–3063

17. Yoon MK, Heider D, Gillespie JW Jr, Ratcliffe CP, Crane RM (2010) Local damage detection with the global fitting method using operating deflection shape data. J Nondestruct Eval 29(1):25–37

18. Feng DM, Feng MQ (2016) Output-only damage detection using vehicle-induced displacement response and mode shape curvature index. Struct Control Health Monit 23(8):1088–1107

19. Sun SH, Jung HJ, Jung HY (2013) Damage detection for beam-like structures using the normalized curvature of a uniform load surface. J Sound Vib 332(6):1501–1519

20. Zhao JH, Zhang L (2012) Structural damage identification based on the modal data change. Int J Eng Man 4:59–66

21. Capecchi D, Ciambella J, Pau A, Vestroni F (2016) Damage identification in a parabolic arch by means of natural frequencies, modal shapes and curvatures. Meccanica 51:2847–2859

22. Ay AM, Khoo S, Wang Y (2019) Probability distribution of decay rate: a statistical time-domain damping parameter for structural damage identification. Struct Health Monit 18(1):66–86

23. Mustafa S, Matsumoto Y, Yamaguchi H (2017) Vibration- based health monitoring of an existing truss bridge using energy-based damping evaluation. J Bridge Eng 23(1):04017114

24. Sampaio RPC, Maia MM, Silva MM (1999) Damage detection using the frequency response- function curvature method. J Sound Vib 226(5):1029–1042

25. Catbas FN, Brown DL, Aktan E (2006) Use of modal flexibility for damage detection and condition assessment: case studies and demonstrations on large structures. J Struct Eng 132(11):1699–1712

26. Dilena M, Morassi A (2011) Dynamic testing of a damaged bridge. Mech Syst Signal Process 25:1485–1507

27. Salawu OS (1997) Detection of structural damage through changes in frequency: a review. Eng Struct 19(9):718–723

28. Avci O, Abdeljaber O, Kiranyaz S, Hussein M, Gabbouj M, Inman DJ (2021) A review of vibration-based damage detection in civil structures: from traditional methods to machine learning and deep learning applications. Mech Syst Signal Process 147:107077

29. Jian-Yu Y, Bin-Hua X, Zengshun C, Tina-Long L, Renming L (2020) Vibration-based structural damage identification: a review. Int J Robot Autom 35(2):123–131

30. Koo KY, Sung SH, Park JW, Jung HJ (2010) Damage detection of shear buildings using deflections obtained by modal flexibility. Smart Mater Struct 19(11):115026

31. Koo KY, Sung SH, Jung HJ (2011) Damage quantification of shear buildings using deflections obtained by modal flexibility. Smart Mater Struct 20(4):045010

32. Sung SH, Koo KY, Jung HY, Jung HJ (2012) Damage-induced deflection approach for damage localization and quantification of shear buildings: validation on a full-scale shear building. Smart Mater Struct 21(11):115013

33. Bernagozzi G, Mukhopadhyay S, Betti R, Landi L, Diotallevi PP (2018) Output-only damage detection in buildings using proportional modal flexibility-based deflections in unknown mass scenarios. Eng Struct 167:549–566

34. Wang Y, Thambiratnam DP, Chan THT, Nguyen A (2018) Method development of damage detection in asymmetric buildings. J Sound Vib 413:41–56

35. Wang Y, Thambiratnam DP, Chan THT, Nguyen A (2018) Damage detection in asymmetric buildings using vibration-based techniques. Struct Control Health Monit 25:e2148. https://doi.org/10.1002/stc.2148

36. Artemis [Computer Software] (2018) Structural vibration solutions. NOVI Science Park, Aalborg

37. FEMA (1998) Evaluation of earthquake-damaged concrete and masonry wall buildings: basic procedures manual. In: FEMA 306, Prepared by the Applied Technology Council (ATC-43 Project), for the Federal Emergency Management Agency, Washington, DC

38. Maeda M, Matsukawa K, Ito Y (2014) Revision of guideline for post–earthquake damage evaluation of RC buildings in Japan. In: Tenth U.S. national conference on earthquake engineering frontiers of earthquake engineering, July 21–25, Anhorage, Alaska

39. SARA electronic instruments s.r.l. (2018) Acebox digital accelerograph (consisted of triaxial force balance accelerometer model. In: SA10 3D and 24 Bit Seismic Digitiser/Recorder Model SL06), Perugia, Italy

40. Ibrahim SR (1977) Random decrement technique for modal identification of structures. J Spacecr Rocket 14(11):696–700

41. Brincker R, Zhang L, Andersen P (2000) Modal identification from ambient responses using frequency domain decomposition. In: Proceedings of the 18th international modal analysis conference, 7–10 February, San Antonio, TX, USA

42. Altunişik AC, Karahasan OŞ, Genç AF, Okur FY, Günaydin M, Kalkan E, Adanur S (2018) Modal parameter identification of RC frame under undamaged, damaged, repaired and strengthened conditions. Measurement 124:260–276

43. Sevim B, Bayraktar A, Altunışık AC, Atamtürktür S, Birinci F (2011) Finite element model calibration effects on the earthquake response of masonry arch bridges. Finite Elem Anal Des 47:621–634

44. Altunışık AC, Bayraktar A, Sevim B, Özdemir H (2011) Experimental and analytical system identification of Eynel arch type steel highway bridge. J Constr Steel Res 67:1912–1921

45. Catbas FN, Susoy M, Frangopol DM (2008) Structural health monitoring and reliability estimation: long span truss bridge application with environmental monitoring data. Eng Struct 30(9):2347–2359

46. Yuen KV, Kuok SC (2010) Ambient interference in long-term monitoring of buildings. Eng Struct 32(8):2379–2386

47. Ni YC, Alamdari MM, Ye XW, Zhang FL (2021) Fast operational modal analysis of a single-tower cable-stayed bridge by a Bayesian method. Measurement 174:109048

48. Gonzalez WM, Boroschek RL, Bilbao JA (2021) Temperature measurement assisted modal tracking of an instrumented building. Eng Struct 233:111907

49. Aras F (2024) Effects of aöbient temperature and magnitude of the vibration on the dynmaics of pre-stressed precast isolated bridges. Turk J Civ Eng 35(1):23–40. https://doi.org/10.18400/tjce.1223515

50. Aras F (2016) Ambient and forced vibration testing with numerical identification for RC buildings. Earthq Struct 11(5):809–822

51. IBC (2000) International building code. International Code Council, Virginia

52. Minimum design loads for buildings and other structures (2010). In: ASCE/SEI 7–10. American Society of Civil Engineers, Reston

53. Allemang RJ (2003) The modal assurance criterion—twenty years of use and abuse. Sound Vib 37(8):14–23